

# Gl 86 B: a white dwarf orbits an exoplanet host star

M. Mugrauer<sup>1\*</sup> and R. Neuhauser<sup>1\* †</sup>

<sup>1</sup>*Astrophysikalisches Institut, Universität Jena, Schillergäßchen 2-3, 07745 Jena, Germany*

Accepted , Received

## ABSTRACT

In this letter we present our first high contrast NACO/SDI observations of the exoplanet host star Gl 86 and results from NACO spectroscopy. Els et al. (2001) found a faint co-moving companion located only  $\sim 2$  arcsec east of the exoplanet host star Gl 86 A. Our high contrast SDI observations rule out additional stellar companions from 1 AU up to 23 AU, and are sensitive for faint T dwarf companions down to  $35 M_{Jup}$ . We present evidence for orbital motion of Gl 86 B around the exoplanet host star Gl 86 A, which finally confirms that this is a bound binary system. With the given photometry from Els et al. (2001) and the obtained NACO spectroscopy we prove that the companion Gl 86 B is a cool white dwarf with an effective temperature of  $5000 \pm 500$  K. This is the first confirmed white dwarf companion to an exoplanet host star and the first observational confirmation that planets survive the post main sequence evolution of a star from which they are separated by only one to two dozen AU (giant phase and planetary nebula) as expected from theory.

**Key words:** stars: individual: Gl 86, stars: binaries: visual, white dwarfs, planetary systems

## 1 INTRODUCTION

Gliese 86 (thereafter Gl 86) is a K1 dwarf located at a distance of  $10.9 \pm 0.08$  pc (Hipparcos, ESA 1997). Queloz et al. (2000) found a 15.8 day periodical variation of its radial velocity. Because Gl 86 does not show any chromospheric activity or photometric variability they concluded that the variation of the radial velocity is induced by an exoplanet with a minimum mass of  $4 M_{Jup}$  on an almost circular orbit ( $e=0.046$ ,  $a=0.11$  AU). Furthermore they reported a long-term linear trend in the radial velocity data ( $0.5 \text{ m s}^{-1} \text{ d}^{-1}$ ) observed over a time span of 20 years in the CORAVEL program and also confirmed by CORALIE measurements ( $0.36 \text{ m s}^{-1} \text{ d}^{-1}$ ). This is a clear signature of a further stellar companion in the Gl 86 system with a period longer than 100 yr ( $a \geq 20$  AU).

Els et al. (2001) found a faint companion 2 arcsec east of Gl 86 which clearly shares common proper motion. They also obtained near infrared photometry ( $J=14.7 \pm 0.2$ ,  $H=14.4 \pm 0.2$ , and  $K=13.7 \pm 0.2$ ) and from the derived color ( $J-K \sim 1$ ) they concluded that Gl 86 B must be substellar with a spectral type between late L to early T. However a sub-

stellar companion ( $m \leq 78 M_{Jup}$ ) cannot explain the detected long term trend in the radial velocity of the exoplanet host star.

At the begin of 2005 we started a search for faint substellar companions of all exoplanet host stars known to harbor several substellar companions, i.e. several planets or as in the case of Gl 86 one planet and a reported brown dwarf companion (see Els et al. 2001). Our goal is to detect additional companions. We carry out our observations with NACO/VLT and its new simultaneous differential imaging device SDI which is particular sensitive for faint cool substellar companions exhibiting strong methane absorption features (T dwarfs), yielding a much higher contrast than standard AO imaging with NACO alone. All our targets are main-sequence stars with ages in the range of 1 to 10 Gyrs. From theoretical models (Baraffe et al. 2003) we expected that most of the substellar companions of our targets are T dwarfs cooler 1400 K, which are detectable with NACO/SDI close to the primary stars.

In section 2 we describe our SDI observations, the obtained astrometry and photometry in detail. With the achieved high contrast SDI imaging we furthermore proof that there is no further companion in the system which could induce the reported long term trend in the radial velocity of Gl 86 A (Queloz et al. 2000). Spectra of Gl 86 B were taken with NACO and were retrieved from the ESO public archive, yielding the surprising result that this companion is a white dwarf companion. We presented the spectroscopy in section

\* E-mail: markus@astro.uni-jena.de (MUG) and rne@astro.uni-jena.de (NEU)

† Based on observations obtained at the European Southern Observatory on Paranal in ESO programs 074.C-0262(A) and 070.C-0179(A), the latter taken from the public archive.

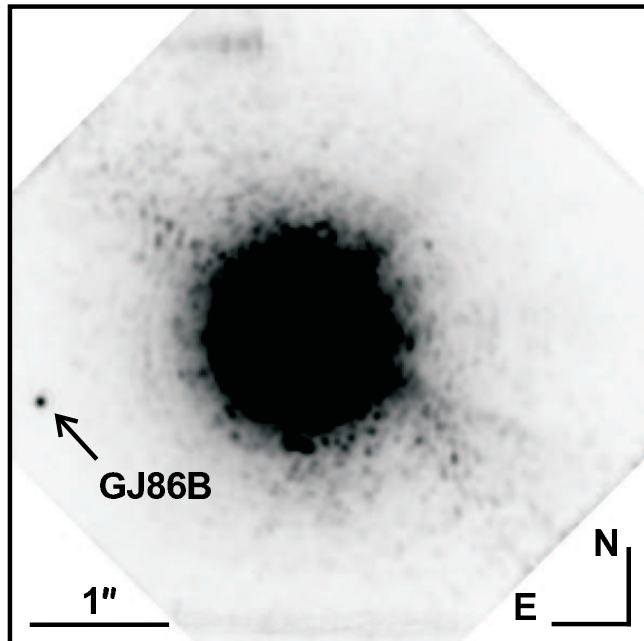


**Figure 1.** 40 min of H band imaging with SDI at the ESO VLT (north up east to the left). This image is taken through the SDI narrow band filter with a central wavelength of  $1.575 \mu\text{m}$ . It is one out of four simultaneously taken images. The bright star in the center is the exoplanet host star GJ86 A. The about 10 mag fainter companion GJ86 B is located  $\sim 2$  arcsec east of the primary. Several bright speckles are clearly visible close to the primary star.

3. Finally section 4 summarizes and discusses all results of this letter.

## 2 NACO/SDI OBSERVATIONS

Detection of faint objects close to a much brighter source is the main challenge in the direct imaging search for substellar companions (brown dwarfs or planets) of stars. Within 1 arcsec of the bright central source the field is filled with speckles which are residuals from the none perfect adaptive optics correction of the incoming disturbed wavefront. The achievable signal to noise in this speckle-noise limited region does not increase with integration time, hence only a subtraction of the speckle pattern can improve the detection limit close to a bright source.

At the ESO/VLT the simultaneous differential imager (SDI) is offered for the AO-system NACO (Lenzen et al. 2004). Therein a double Wollaston prism splits the beam, coming from the AO system, into 4 beams which pass then through three different narrow band filters with central wavelengths  $1.575$ ,  $1.600$  and  $1.625 \mu\text{m}$  and a bandwidth of  $25 \text{ nm}$  bandwidth each. The resulting speckle pattern of the four images is almost identical. Since cool ( $T \leq 1400 \text{ K}$ ) objects exhibit a strong methane absorption band at  $1.62 \mu\text{m}$  they appear much fainter in the  $1.625 \mu\text{m}$  filter than in the  $1.575 \mu\text{m}$  filter while the bright star and therefore also the speckle pattern has roughly equal brightness in all images. Subtracting the  $1.625 \mu\text{m}$  SDI image from the image taken through the  $1.575 \mu\text{m}$  SDI filter will effectively cancel out the speckle pattern of the star while the signal from the cool companion remains (see e.g. Biller et al. 2004).

We observed GJ86 on 12. Jan 2005 with SDI (see Fig. 1). Due to the small SDI field of view ( $5 \times 5$  arcsec, tilted by  $45^\circ$ ), jittering cannot be used for background subtraction. However we apply a small jitter with a box width of only  $0.2$  arcsec (10 SDI pixel) to correct for bad pixels. Per jitter cycle 5 object frames are taken, each is the average of 60 exposures of  $2 \text{ s}$  each. We always adjust the individual integration time so that only the central 9 SDI pixel of the primary point spread function are saturated. This improves the detection limit for faint companions at larger separations to the primary. At the end of each jitter cycle a sky-frame ( $10$  arcsec offset from the target in Ra and Dec) is taken which is then subtracted from the 5 object frames to cancel out the bright infrared sky background. The sky-frames are taken in the same way as the the target-frames, i.e. 60 times  $2 \text{ s}$  integrations. The jitter cycle is repeated 4 times which yields a total on source integration time of  $40 \text{ min}$ . To distinguish between faint companions and any residual speckles we observe each target at the detector position angles  $0$  and  $33^\circ$ , i.e.  $2 \times 40 \text{ min}$  integration time in total.

For infrared data-reduction we use the ESO *Eclipse* package. After flatfielding, we extract the four SDI quadrants (left-top  $1.6 \mu\text{m}$ , right-top  $1.575 \mu\text{m}$ , bottom both quadrants  $1.625 \mu\text{m}$ ) and apply image-registration, shifting, and final averaging on all individual frames. Because the radial position of the speckles is proportional to the wavelength all SDI images must be spatially rescaled. Finally the images are aligned, and their flux is adjusted to eliminate any differences in the quantum efficiency. The  $1.575 \mu\text{m}$  and the  $1.625 \mu\text{m}$  images (top-right and bottom-left quadrant) follow the same path through the SDI instrument, i.e. they provide very similar speckle pattern and yield the best contrast for methane rich companions. We therefore subtract these two SDI images. The difference frame taken at position angle  $0^\circ$  is then subtracted from the difference frame taken at position angle  $33^\circ$ . To filter out low spatial frequencies all frames are unsharp masked (see Fig. 2). The resulting difference frame compared to the image taken at  $1.575 \mu\text{m}$  is shown in Fig. 2. The speckle pattern is effectively subtracted and a detection limit of  $12.8 \text{ mag}$  is reached at a separation of  $0.5$  arcsec.

For astrometrical calibration of the SDI camera we observed the binary HIP 9487. This system is listed in the Hipparcos catalogue ( $\rho = 1.876 \pm 0.001$  arcsec and  $\theta = 278.500 \pm 0.001^\circ$  at epoch 1991.25) and accurate astrometry is available for both components. Therefore the binary separation and position angle can be computed for the given observing epoch (12 Jan. 2005). We derive a pixelscale of  $17.210 \pm 0.087 \text{ mas}$  per pixel. The true north is slightly rotated to the east by  $0.33 \pm 0.24^\circ$ .

Due to the large proper and parallactic motion of GJ86 ( $\mu_\alpha \cos(\delta) = 2092.59 \pm 0.56 \text{ mas/yr}$ ,  $\mu_\delta = 654.49 \pm 0.49 \text{ mas/yr}$ , and  $\pi = 91.63 \pm 0.61 \text{ mas}$ , Hipparcos ESA 1997) Els et al. (2001) already proved that GJ86 A and B form a common proper motion pair, a result which is significantly ( $263\sigma$  in separation and  $279\sigma$  in position angle) confirmed with our SDI observations (see Fig. 3). GJ86 B is located  $1.93 \pm 0.01$  arcsec at a position angle of  $104.0 \pm 0.3^\circ$ . Fig. 3 illustrates the astrometry from Els et al. (2001) and our astrometric results. The expected change of separation and position angle is calculated assuming that only GJ86 A

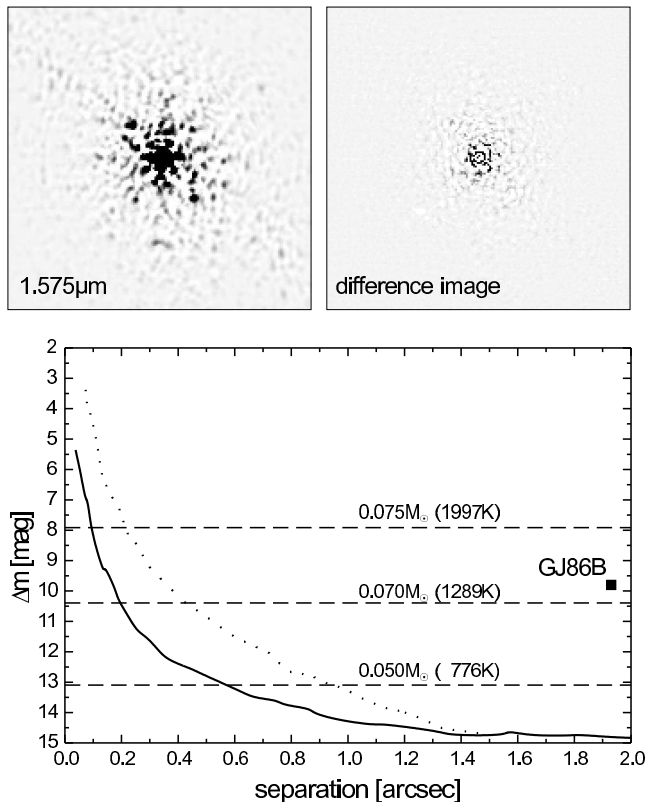


**Figure 2.** The upper left pattern shows the central part of Fig. 1 (2.8 arcsec box width). The detection limit for this image is illustrated as a dotted line in the bottom panel. The right pattern shows the subtraction of the difference images (1.575-1.625  $\mu\text{m}$ ) taken at detector position angle 0 and 33°. The speckle pattern is effectively subtracted and the achieved detection limit is improved close to the primary (see solid line). A magnitude difference of 12.8 mag is reached at 0.5 arcsec, which is 5.5 AU in projected separation. The dashed horizontal lines illustrate the expected magnitude differences for substellar companions derived with Baraffe et al. (2003) COND models, assuming a system age of 10 Gyrs. All stellar companions can be detected beyond 0.1 arcsec, i.e. 1 AU in projected separation and T dwarfs come into range beyond 0.2 arcsecs (2 AU). We are sensitive for substellar companions down to  $35 M_{\text{Jup}}$

. G186 B is well detected in our SDI images and is shown as a black square.

is moving and G186 B is an unrelated background star (see dashed lines in Fig. 3).

By comparing our astrometry with data from Els et al. (2001) we find a significant change in position angle of  $-15.5 \pm 0.5^\circ$  and  $+0.196 \pm 0.024$  arcsec in separation for the given epoch difference. This is a clear evidence for orbital motion. The expected orbital motion for a companion at a separation of 21 AU is shown with dotted lines in Fig. 3 (0.090 arcsec/yr and  $4.2^\circ$ /yr, see also section 4).

With the J,H and K infrared magnitudes of G186 B given by Els et al. (2001) and the Hipparcos parallax of G186 A we derive the absolute magnitudes of G186 B:  $M_J = 14.5 \pm 0.2$  mag,  $M_H = 14.2 \pm 0.2$  mag,  $M_K = 13.5 \pm 0.2$  mag. If we assume that G186 B is a brown dwarf companion these absolute magnitudes are consistent with a spectral type L7 to T5 (see Vrba et al. 2004). In our SDI images G186 B is comparable bright in all three fil-

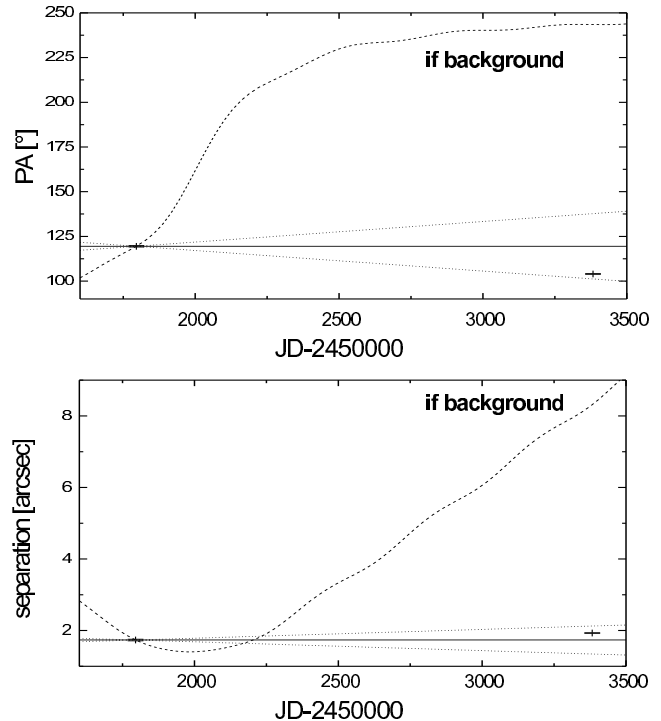


**Figure 3.** This plot illustrates the astrometric results for the G186 A/B system. The first data point is taken from Els et al. (2001) for epoch 2000. Our SDI astrometry significantly confirms the common proper motion of G186 B to its primary. The dashed lines illustrate the expected change in position angle and separation if only G186 A is moving and G186 B is a none-moving background source. The dotted lines show the expected orbital motion.

ter. We measure flux-ratios  $F_{1.575 \mu\text{m}}/F_{1.625 \mu\text{m}} = 1.11 \pm 0.04$ . This clearly rules out spectral types later than T3, because for these spectral types  $F_{1.575 \mu\text{m}}/F_{1.625 \mu\text{m}} > 1.3$  due to methane absorption.

### 3 NACO SPECTROSCOPY

Infrared spectra of G186 B were taken in ESO observing program 070.C-0173(A) (extracted by us from the public archive). 8 spectra (120 s each) were taken in spectroscopic mode S27-SK-3 using the 86 mas slit, which yields a resolving power  $\lambda/\Delta\lambda = 1400$ . For background subtraction, 8 arcsec nodding was applied along the slit. To avoid that the bright primary is located on or close to the slit (saturation) the slit was orientated perpendicular to the position vector of G186 B relative to the primary. All images are flatfielded (lamp flats) and the spectra are extracted, wavelength calibrated (with Argon lines) and finally averaged, with standard routines in IRAF. The resulting spectrum is flux calibrated with the photometric standard HIP 020677 (G2V). Figure 4 shows the flux calibrated NACO spectrum of G186 B, together with spectra of M1, L5, and T5 dwarfs from Cushing et al. (2005). For the given spectral range the achieved signal to noise is  $\sim 40$ . Neither characteristic molecular nor atomic absorption features are visible and the continuum is clearly different to those of L and T dwarfs. The spectrum is even steeper than the M1V reference spectrum

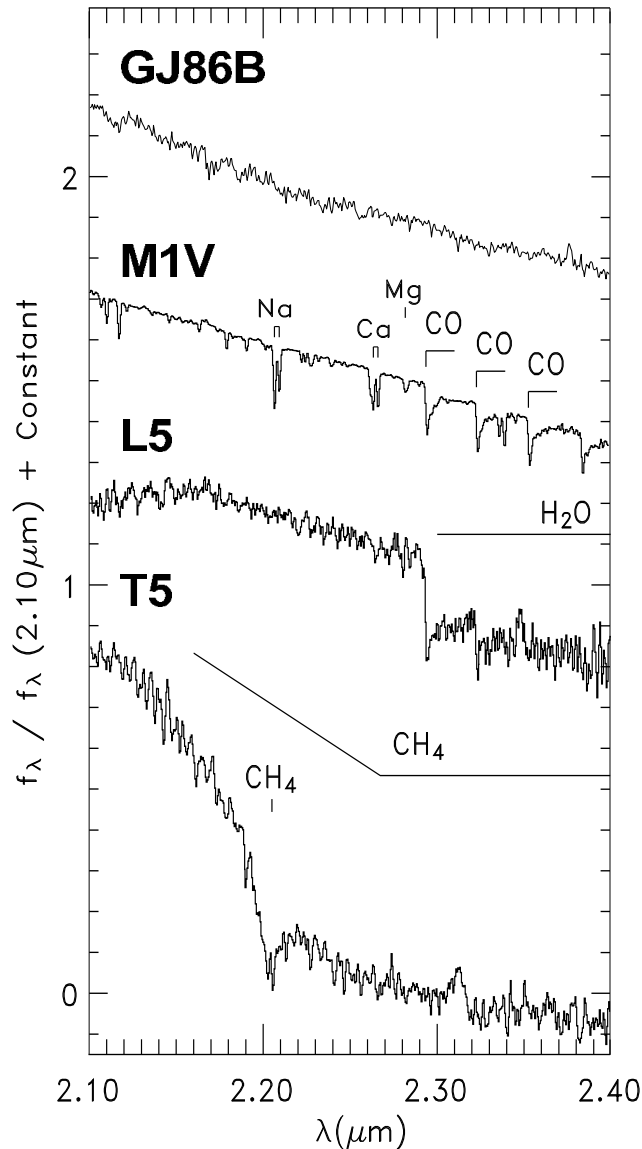


**Figure 4.** The NACO K band spectrum of G186 B with comparison M1V, L5, and T5 comparison spectra of cool dwarfs from Cushing et al. (2005).

which points to an effective temperature hotter than 3700 K. However, in the K-band, the gradient of the continuum is only slightly varying for effective temperatures higher than 4000 K, so that we can only give a low temperature limit for G186 B.

Therefore we conclude that G186 B is a cool white dwarf companion (see Fig.5). Due to its high surface gravity ( $\log(g) > 7$ ) all absorption lines are strongly broadened and therefore hardly detectable (see e.g. Br  $\gamma$  absorption line at  $2.17 \mu\text{m}$ , in Dobbie et al. 2005). We compare the absolute infrared photometry of G186 B with data from Bergeron et al. (2000), who carried out a detailed photometric and spectroscopic analysis of cool white dwarfs, and derive an effective temperature of  $5000 \pm 500 \text{ K}$ .

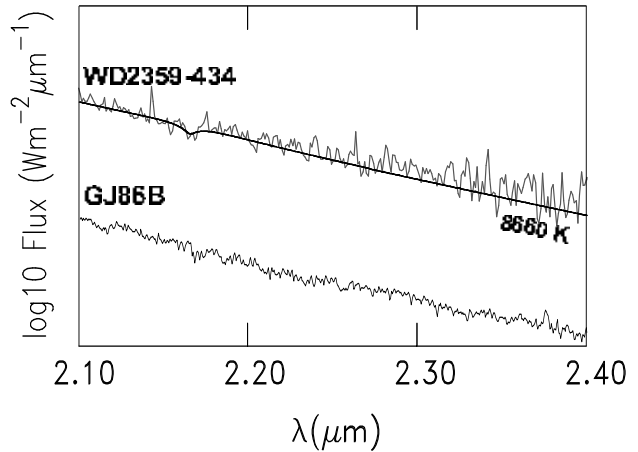


**Figure 5.** The NACO K band spectrum of G186 B with a comparison white dwarf spectra from Dobbie et al. (2005).

#### 4 CONCLUSIONS

We confirmed common proper motion of G186 B to its primary and detected its orbital motion. This is a clear evidence that G186 B is a bound companion of the exoplanet host star with a projected separation of 21 AU ( $1.93 \pm 0.01$  arcsec). With the achieved high contrast SDI detection limit we can rule out any further stellar companions beyond 0.1 arcsec up to 2.1 arcsec, i.e. 1 AU to 23 AU in projected separation. T dwarf companions ( $T < 1400 \text{ K}$ ) can be detected beyond 0.2 arcsecs (2 AU) and we are sensitive for faint substellar companions down to  $35 M_{Jup}$ . The NACO spectrum of G186 B is clearly different to the expected spectral type between L5 and T5 derived from infrared photometry. G186 B is faint but its spectrum implies that it is even hotter than 3700 K (M1). Therefore we conclude that G186 B is a cool white dwarf companion.

Queloz et al. (2000) report a long-term trend in the radial-velocity data of G186 A ( $0.5 \text{ m s}^{-1} \text{ d}^{-1}$ ). This is a clear hint on a further stellar companion in the G186 system. We compute that with a separation of 21 AU, the mass of G186 B must be  $0.55 M_{\odot}$  to induce this trend in the radial velocity. The derived mass is well consistent with a white dwarf companion. Santos et al. (2004) determined the mass of G186 A to be  $0.7 M_{\odot}$ , hence the total mass of the system is  $1.25 M_{\odot}$  and with a binary semi-major axis of 21 AU, the expected orbital time is 86 yr. This yields an orbital motion of  $0.090 \text{ arcsec/yr}$  and  $4.2^{\circ}/\text{yr}$ , assuming a circular orbit, which is also consistent with the measured orbital motion (see Fig. 3).

If we assume that both components of the binary have the same age, the white dwarf progenitor must be more massive than G186 A ( $0.7 M_{\odot}$ ) to be observable today as a white dwarf companion. According to Weidemann (2000) a  $0.55 M_{\odot}$  white dwarf is the remnant of  $1 M_{\odot}$  star. With the white dwarf models presented by Richer et al. (2000) and the derived effective temperature of G186 B ( $5000 \pm 500 \text{ K}$ ) we can approximate a cooling timescale between 3 and 6 Gyr, i.e. the binary system should be 13 to 16 Gyrs old. For more massive white dwarf progenitors ( $2-4 M_{\odot}$ ) the system age ranges between 2 to 8 Gyr.

G186 B is the first confirmed white dwarf companion

to an exoplanet host star. Theoretically, planets may or may not survive the red giant and asymptotic giant branch phases of stellar evolution. Planets which are located outside the red giant's envelope, which reaches about a few hundred solar radii will survive. Closer companions will be either destroyed or migrate inward and become a close companion to the white dwarf remnant. According to Burleigh et al. (2002) it seems likely that distant planets ( $a > 5$  AU) survive the late stages of stellar evolution of main-sequence stars with masses in the range between 1 and  $8 M_{\odot}$ , i.e. all white dwarf progenitors. In particular in the Gl 86 system the separation between the white dwarf and the exoplanet (21 AU) is large enough that it seems very well possible that the planet can survive the post main sequence phase of a F or G dwarf.

Furthermore we should mention that Gl 86 is one of the closest binaries known today to harbor an exoplanet. Only two other systems  $\gamma$  Ceph ( $a \sim 19$  AU,  $e \sim 0.36$ , see Hatzes et al. 2003) and HD 41004 (23 AU see Zucker et al. 2004) have comparable separations. In such close binary systems the dynamical stability of planets is limited to a small region around the planet host star. According to Holman & Wiegert (1999) the critical semi-major axis  $a_c$  for planets around Gl 86 A is only 6.2 AU assuming a circular binary orbit ( $m = 0.55 M_{\odot}$  and  $a = 21$  AU). Due to mass loss during the post main sequence phase of the white dwarf progenitor, the binary separation was even smaller before ( $M_{\text{tot}} a = \text{const} \rightarrow a_{\text{old}} = 15.4$  AU), i.e.  $a_c = 3.7$  AU. We calculate critical semi-major axis also for the two other close binaries and get  $a_c = 7.5$  AU for HD 41004 and  $a_c = 4.0$  AU for  $\gamma$  Ceph. We should mention that all exoplanets detected in these close binary systems actually reside within the proposed long-time stable regions. However it would be of particular interest to search for further substellar companions in these close binaries to verify with observational results the published theoretical constraints of planet stability in binary systems.

## REFERENCES

Baraffe I., Chabrier G., Barman T. S., Allard F., Hauschildt P. H., 2003, *A&A*, 402, 701  
 Bergeron P., Leggett S. K. & Ruiz M. T., 2001, *ApJS*, 133, 413  
 Biller B. A., Close L., Lenzen R., Brandner W., McCarthy D. W. et al., 2004, *SPIE*, 5490, 389  
 Burleigh, M. R., Clarke, F. J., Hodgkin, S. T., 2002, *MNRAS*, 331, 41  
 Cushing M. C., Rayner J. T. & Vacca W. D., 2005, *ApJ*, astro-ph/0412313  
 Dobbie P. D., Burleigh M. R., Levan A. J., Barstow M. A., Napiwotzki, R. et al., 2005, *MNRAS*, 83  
 Els S. G., Sterzik M. F., Marchis F., Pantin E., Endl M. et al., 2001, *A&A*, 370, 1  
 Hatzes A. P., Cochran W. D., Endl M., McArthur B., Paulson D. B. et al., 2003, *ApJ*, 599, 1383  
 Holman M. J., Wiegert P. A., 1999, *AJ*, 117, 621  
 Lenzen R., Close L., Brandner W., Biller B., Hartung M., 2004, *SPIE*, 5492, 970  
 Queloz D., Mayor M., Weber L., Blécha A., Burnet M et al., 2000, *A&A*, 354, 99

Richer H. B., Hansen B., Limongi M., Chieffi A. Straniero O. et al., 2000, *ApJ*, 529, 318  
 Santos N. C., Israelian G., Mayor M., 2004, *A&A*, 415, 1153  
 Vrba F. J., Henden A. A., Luginbuhl C. B., Guetter H. H., Munn, J. A. et al., 2004, *AJ*, 127, 2948  
 Weidemann V., 2000, *A&A*, 363, 647  
 Wood M. A., 1992, *ApJ*, 386, 539  
 Zucker S., Mazeh T., Santos N. C., Udry, S., Mayor M., 2004, *A&A*, 426, 695